VENTING DEFLAGRATIONS OF LOCAL HYDROGEN-AIR MIXTURE

Makarov, D.[1], Molkov, V.[1], Hooker, P.[2] and Kuznetsov, M.[3]
[1] HySAFER Centre, University of Ulster, Newtownabbey, BT37 0QB, UK
[2] Health and Safety Laboratory, Harpur Hill, Buxton, SK17 9JN, UK
[3] Karlsruhe Institute of Technology, 76344 Eggenstein-Leopoldshafen, Germany
dv.makarov@ulster.ac.uk

ABSTRACT

The paper describes a lumped-parameter model for vented deflagrations of localised and layered fuel-air mixtures. Theoretical model background is described to allow insight into the model development with focus on lean mixtures and overpressures significantly below 0.1 MPa for protection of low-strength equipment and buildings. Phenomena leading to combustion augmentation was accounted based on conclusions of recent CFD studies. Technique to treat layered mixtures with concentration gradient is demonstrated. The model is validated against 25 vented deflagration experiments with lean non-uniform and layered hydrogen-air mixtures performed in Health and Safety Laboratory (UK) and Karlsruhe Institute of Technology (Germany).

NOMENCLATURE

A_S	area of the sphere with volume equal to burnt mixture volume (m^2)
A	fraction of vent area occupied by combustion products, or correlation coefficient in (10)
a	characteristic length of enclosure (m)
B	correlation coefficient in (10)
Br_t	turbulent Bradley number, $Br_t = \left(\sqrt{E_i/\gamma}\,\mu F c_{ui}\right)/\left((36\pi_0)^{1/3}\chi V^{2/3} S_{ui}(E_i-1)\right)$
c_{ui}	speed of sound in unburnt mixture (m/s),
D	fractal dimension
E_i	expansion ratio, $E_i = \rho_{ui}/\rho_{bi}$
F	vent area (m^2)
G	mass flow rate (kg/s)
H	height (m), or enthalpy (J)
L	length (m)
M	molecular mass (g/mol)
m	mass (kg), or temperature index for burning velocity
n	mass fraction, or burning velocity baric index
p	pressure (Pa abs)
R	flame radius (m), or universal gas constant, R=8314 (J/K/kmol)
$R^{\#}$	non-dimensional parameter, $R^{\#} = \left\{(2\gamma)/(\gamma-1)\pi_m\sigma\left[(1/\pi_m)^{2/\gamma_u} - (1/\pi_m)^{1+1/\gamma_u}\right]\right\}^{1/2}$
R_0	critical radius for transition to fully turbulent flame propagation regime (m)
S_t	turbulent burning velocity (m/s)
S_u	laminar burning velocity (m/s)
T	temperature (K)
t	time (s)
U	internal energy (J)
V	volume (m^3)
W	width (m), or non-dimensional ventilation parameter, $W = \mu F c_{ui}/\left[(36\pi_0)^{1/3}\sqrt{\gamma_u}V^{2/3}S_{ui}\right]$, or mechanical work of gas (J)
x_{H2}	volume faction of hydrogen in entire enclosure, $x_{H2} = \varphi\cdot\Phi$
Y	mass fraction
Z	non-dimensional number $Z = \gamma_b\left[E_i - (\gamma_u/\gamma_b)(\gamma_b-1)/(\gamma_u-1)\right]\pi^{(1-\gamma_u)/\gamma_u} + (\gamma_u-\gamma_b)/(\gamma_u-1)$

Greek

χ	turbulence (flame wrinkling) factor
Φ	volume fraction of localised combustible fuel-air mixture (or layer) in enclosure
γ	specific heat ratio
φ	volume fraction of fuel in localised fuel-air mixture
μ	vent discharge coefficient
ν	specific volume, (m^3/kg)
π	non-dimensional pressure $\pi = p/p_i$
π_0	π_0=3.14159
χ/μ	deflagration-outflow interaction number
Ψ	empirical coefficient
Ξ_K	wrinkling factor to account for turbulence generated by the flame front itself
Ξ_{LP}	wrinkling factor to account for leading point flame acceleration mechanism
Ξ_{FR}	wrinkling factor to account for fractal increase of flame surface area
$\Xi_{u'}$	wrinkling factor to account for initial flow turbulence
Ξ_{AR}	wrinkling factor to account for aspect ratio of the enclosure
Ξ_O	wrinkling factor to account for the presence of obstacles
ρ	density (kg/m^3), $\rho = pM/(RT)$
σ	relative density, $\sigma = \rho/\rho_i$
τ	non-dimensional time, $\tau = t\,S_{ui}/a$
ω	volume fraction

Superscripts

‘	value in fuel-air mixture

Subscripts

air	air
b	burnt mixture
corr	correlation value
exp	experimental value
f	fuel
H2	hydrogen
i	initial conditions
MAX	maximum
MIN	minimum
t	turbulent
u	unburned mixture

Acronyms

BOS	Background Oriented Schlieren technique
CFD	Computational Fluid Dynamics
DOI	Deflagration-Outflow Interaction
LES	Large Eddy Simulation
SGS	Sub-Grid Scale

1.0 INTRODUCTION

Formation and explosion of stratified fuel-air mixtures, where concentration varies only in one direction, is a realistic accident scenario for both industrial environment and domestic premises [1]. It may result from a slow release of flammable heavier or lighter than air gas, or a spill of flammable liquid leading to formation of reactive layer near the floor or ceiling. Combustion behaviour of hydrogen-air-steam mixtures is of interest in the analysis of postulated post-accident nuclear containment events [2, 3]. Mitigation techniques for hydrogen deflagrations are on the research agenda due to the recent increase of commercial efforts to introduce hydrogen as an energy carrier to the market worldwide.

Though venting of stratified or partial-volume (localised) mixture deflagrations is expected to be easier than venting of full-volume mixture explosions, the design against deflagrations of stratified mixtures usually presumes that the entire enclosure volume is occupied by the explosive mixture [1, 4]. On the other hand deflagrations in mixtures with concentration gradient may be more dangerous than those in uniform compositions with the same amount of flammable gas [2]. It was found that characteristic flame velocity and maximum combustion overpressure are governed by the maximum hydrogen concentration at the top of the stratified layer [3-7]. Critical conditions for different flame propagation regimes in layered and stratified mixtures in large scale experiments up to 100 m^3 were investigated at KIT [3,5-7].

First lumped parameter models describing vented explosion dynamics were developed by Yao [9] and Pasman et al. [10]. Detailed gaseous vented deflagration theory was then published by Bradley and Mitcheson [11]. Later an original theory was proposed by Molkov and Nekrasov [12]. Comparative study of a number of vent sizing approaches was performed by Razus and Krause [13]. Recent effort in this field includes work by research groups at FM Global, e.g. [1,14,15], and at Ulster, e.g. [4,16,17]. Comparison of some modelling approaches for simulation of hydrogen-air deflagrations can be found in [18], where it was noted that the vented deflagration correlation in NFPA68 "Guide for venting of deflagrations" [19] is not able to predict overpressure for hydrogen-air mixtures. For the best of authors' knowledge the analytical and semi-empirical correlations for the vented deflagration overpressure developed to the date do not address localised mixture deflagrations.

The aim of the paper is to demonstrate model development for a vented localised fuel-air mixture deflagrations. The model for vented localised mixture deflagration is validated against experiments with stratified (layered) hydrogen-air compositions with and without concentration gradient performed in 1 m^3 experimental facility at Karlsruhe Institute of Technology (KIT), Germany, and 31.25 m^3 facility at Health and Safety Laboratory (HSL), UK.

2.0 EXPERIMENTAL PROGRAMME AND EXPERIMENTAL FACILITY

2.1 Experimental programme at Karlsruhe Institute of Technology

The vented chamber at KIT had nearly cubic shape with dimensions $H \times W \times L$ = 1000×960×980 mm^3. The vessel was located in a room having sizes 5.5×8.5×3.4 m (160 m^3 volume). Rear, bottom and front panels were manufactured of 10 mm thick aluminium plate. The top, left and right vessel walls were fabricated of optically transparent sandwich panels (5 mm thick fire-resistant glass and 15 mm thick plexiglas on the outer side) to provide optical access and video record of deflagration process. Background Oriented Schlieren (BOS) technique was used to detect flame front location based on visualisation of density gradients, for which a random background pattern was fixed behind the experimental vessel. The vent was covered using stretched latex membrane during the mixture preparation procedure. To avoid the effect of membrane on deflagration dynamics, it was cut open using electrically driven knife prior to ignition.

The experimental programme with uniform layered mixtures included hydrogen vol. fractions φ =0.10, 0.15, 0.20 and 0.25, unburnt mixture vol. fractions Φ=0.25 and 0.50, and a square vent of constant area 0.25 m^2. Experiments with non-uniform layer composition included six different gradient layers (referred as Gradient 1 – Gradient 6) with maximum hydrogen fraction from φ =0.10 to 0.20, and vent areas 0.01 and 0.25 m^2. Details of hydrogen distribution in non-uniform layers are given in a following section.

Hydrogen-air mixture with specified hydrogen concentration was prepared in a separate vessel using mass flow controllers. Then the homogenous mixture of predefined concentration was slowly injected into the test chamber close to its ceiling. Thickness of the layer was controlled by the amount of injected mixture replacing air out of the chamber. Hydrogen concentration in the vessel and in the exhaust flow was continuously monitored, and the specified layer of given hydrogen-air mixture was formed when hydrogen concentration at outflow reached that one at the inflow. Hydrogen

concentration was monitored during mixture preparation by sampling probes method combined with Fisher-Rosemount MLT4 gas analyser.

Fast PCB, Kistler and Kulite XTEX pressure sensors were used to measure experimental overpressure (four transducers inside the vessel and five transducers outside of it, two sensors inside and two sensors outside the vessel). Pressure dynamics was recorded using a fast data acquisition system.

Ignition system used spark electrodes and continuous sparking for reliable ignition. A rear top ignition location was used in all experiments with uniform and non-uniform hydrogen-air layers.

2.2 Health and Safety Laboratory explosion box and experiment

A series of large-scale tests with non-uniform mixture layers was conducted at HSL facility. The vented enclosure has geometry similar to many ISO container-based hydrogen facilities with dimensions $H \times W \times L$ =2.5×2.5×5.0 m (volume 31.25 m^3). The enclosure has been located at the test site, fitted with the passive vents and a controlled hydrogen supply. It was designed to withstand an internal explosion overpressure of 0.2 bar. The hydrogen was introduced via vertical pipe installed near the floor with nominal release 150 NL/min. A small hole in the floor was used to avoid over-pressurising the enclosure during the addition of the hydrogen. For the considered experiments with non-uniform mixture layers the deflagrations were vented through two passive vents within the enclosure walls each having area 0.224 m^2. The vents were covered by 20 micron polyethylene sheet pre-perforated around its perimeter to facilitate a "clean" opening of the cover during a deflagration. This arrangement typically gave an opening pressure of approximately 1000 Pa for the relief panels. The mixtures were ignited by a spark plug located at 0.3 m distance from the ceiling and 0.8 m far from a wall opposite to the vents. The ignition source was an AC spark which ran for a few seconds and provided relatively large ignition energy (in excess of 1 J). The hydrogen concentration was analysed by measuring the change in oxygen concentration depletion using electrochemical oxygen sensors, spaced vertically at approximately 0.31 m from each other. Oxygen sensors had accuracy ±0.1% vol., which translated in hydrogen fraction uncertainty about 0.5% vol. The internal pressure was measured using two Kistler pressure transducers mounted flush with the side walls of the enclosure. Unfortunately only one of three conducted tests with stably stratified quiescent gradient mixtures (test WP3/Test22) could be used for the lumped parameter model validation purpose as in the other two maximum deflagration overpressure was equal to the vent opening overpressure, i.e. maximum overpressure was not result of deflagration dynamics but determined by strength of polyethylene cover.

3.0 THEORETICAL MODEL FOR VENTING LOCALISED MIXTURE DEFLAGRATION

3.1 Major derivation steps and assumptions

Conceptual calculation scheme considers a flammable mixture containing fuel with mass m_f and volume V_f, and air with mass m'_{air} and volume V'_{air}. It makes volume fraction of fuel in the combustible mixture $\varphi = V_f / \left(V_f + V'_{air}\right)$ and fraction of fuel-air mixture in the vessel $\Phi = \left(V_f + V'_{air}\right) / \left(V_f + V_{air}\right)$, where V_a is total air volume in the vessel including flammable mixture.

The model was originally developed in [20] and major derivation steps are demonstrated below. At the model core are the following non-dimensional equations: conservation of volume in enclosure

$$\omega_u + \omega_b = 1, \tag{1}$$

equation of mass flow rate through the vent

$$G = \mu F \left\{ \frac{2\gamma}{\gamma - 1} \rho\, p \left(\frac{p_i}{p} \right)^{2/\gamma} \left[1 - \left(\frac{p_i}{p} \right)^{(\gamma-1)/\gamma} \right] \right\}^{0.5}, \tag{2}$$

mass conservation equation for burnt and unburnt mixtures

$$n_b + n_u + \int_0^t \left[\frac{AG_b + (1-A)G_u}{m_i} \right] dt = 1, \tag{3}$$

and conservation equation for internal energy

$$u_i = \int_{n_b} u_b \, dn_b + \int_{n_u} u_u \, dn_u + \int_0^t \left[A\left(u_b + \frac{p}{\rho_b} \right) \frac{G_b}{m_i} + (1-A)\left(u_u + \frac{p}{\rho_u} \right) \frac{G_u}{m_i} \right] dt , \tag{4}$$

where internal energy of burnt and unburnt mixtures are:

$$u_u = u_i + \frac{c_{vu}}{M_u}(T_u - T_{ui}),\ u_b = u_{bi} + \frac{c_{vb}}{M_b}(T_b - T_{bi}) - R\left(\frac{T_{bi}}{M_b} - \frac{T_{ui}}{M_u} \right). \tag{5}$$

Using perfect gas law and assuming the process is adiabatic it may be shown that the non-dimensional energy equation becomes

$$\pi + \gamma_b - 1 = \gamma_b E_i \left(n_b + \int_0^t \frac{AG_b}{m_i} dt \right) + \frac{\gamma_b - \gamma_u}{\gamma_b - 1} \pi^{1-1/\gamma_u} n_u + \tag{6}$$

$$+ \gamma_u \frac{\gamma_u - \gamma_b}{\gamma_u - 1} \left[n_u + \int_0^t (1-A)\left(1 - \pi^{1-1/\gamma_u}\right) \frac{G_u}{m_i} dt \right] - \gamma_b \int_0^t A \pi^{1-1/\gamma_u} \frac{\left(\pi^{1/\gamma_u} - n_u\right)}{n_b} \frac{G_b}{m_i} dt .$$

Burning velocity is introduced via rate equations for unburnt and burnt mixtures, after which the energy equation becomes

$$\frac{d\pi}{d\tau} = \frac{\chi Z \pi^{(\varepsilon+1)/\gamma_u} \left(1 - n_u \pi^{-1/\gamma_u}\right)^{2/3} - \gamma_b W \left[(1-A) R_u^{\#} + A R_b^{\#} \dfrac{\pi^{1/\gamma_u} - n_u}{n_b} \right]}{\left(\pi^{1/\gamma_u} - \dfrac{\gamma_u - \gamma_b}{\gamma_u} n_u \right) \dfrac{1}{3\pi}} . \tag{7}$$

This form of energy equation has a meaning of gas generation-outflow balance for subsonic flows. The following model development is based on a number of assumptions and simplifications:

1. maximum overpressure conditioned by $d\pi/d\tau = 0$,
2. the outflowing gas is entirely fresh mixture and $A = 0$ (conservative assumption),
3. equal adiabatic indexes for fresh and burnt mixtures, $\gamma_b = \gamma_u = \gamma$ (acceptable for lean mixtures),
4. equal molar masses in air and combustible mixture, $M_u \approx M_{air}$ (acceptable for lean mixtures),
5. subsonic regime of gas outflow from enclosure and close to unity non-dimensional pressure $\pi \approx 1.0$ leading to the simplified expression for $R_u^{\#}$: $R_u^{\#} = \left\{ 2\pi(\pi - 1)\sigma_u \right\}^{1/2} = \left\{ 2\pi(\pi - 1)\pi^{1/\gamma} \right\}^{1/2}$.

Substituting appropriate expressions for *Z*, $R_u^{\#}$ and *W*, and taking into account that ω_b cannot be larger than 1.0, leads to $W = \left[\chi (E_i - 1) E_i^{2/3} n_{mi}^{2/3} \pi^{\frac{5-9\gamma}{6\gamma} + \varepsilon} \right] \Big/ \left[2(\pi - 1) \right]^{1/2}$, where the expression $\pi^{(5-9\gamma)/6\gamma + \varepsilon}$ is close to 1.0 for low pressures and lean hydrogen mixtures, and $(\pi - 1) = \Delta\pi$ is the sought-out non-dimensional overpressure. Keeping in mind that the term $E_i^{2/3} n_{mi}^{2/3}$ is the approximate expression of ω_b, which cannot be larger than 1.0, and using the auxiliary relation $m_{air}/m_f = (M_{air}/M_f)\left[1/(\Phi\varphi) - 1\right]$ it may be shown that expression for the relative overpressure of localized mixture vented deflagration is now

$$\Delta\pi = \frac{\left(\chi\left(E_i-1\right)\right)^2}{2\left(\frac{1}{\left(36\pi_0\right)^{1/3}\sqrt{\gamma}}\frac{\mu F}{V^{2/3}}\frac{c_{ui}}{S_{ui}}\right)^2}\cdot MIN\left\{1.0;\left[E_i^{2/3}\left(\frac{1+\left(\frac{1}{\varphi}-1\right)\frac{M_{air}}{M_f}}{1+\left(\frac{1}{\Phi\varphi}-1\right)\frac{M_{air}}{M_f}}\right)^{2/3}\right]^2\right\}, \quad (8)$$

or, bringing into consideration turbulent Bradley number,

$$\Delta\pi = \left(Br_t^{-1}\sqrt{\frac{E_i}{2}}\right)^2\cdot MIN\left\{1.0;\left[E_i^{2/3}\left(\frac{1+\left(\frac{1}{\varphi}-1\right)\frac{M_{air}}{M_f}}{1+\left(\frac{1}{\Phi\varphi}-1\right)\frac{M_{air}}{M_f}}\right)^{2/3}\right]^2\right\}. \quad (9)$$

The experimentally fitted correlation will be sought in the form similar to vented deflagration correlation for uniform mixtures [4,17] $\Delta\pi = A\,Br_t^{-B}$:

$$\Delta\pi = A\,Br_t^{-B}\left(\sqrt{\frac{E_i}{2}}\cdot MIN\left\{1.0;\left[E_i^{2/3}\left(\frac{1+\left(\frac{1}{\varphi}-1\right)\frac{M_{air}}{M_f}}{1+\left(\frac{1}{\Phi\varphi}-1\right)\frac{M_{air}}{M_f}}\right)^{2/3}\right]\right\}\right)^2, \quad (10)$$

where the term in the parenthesis is "additional" compare to the above venting correlation for uniform mixture deflagration. In the limit $\Phi = 1$ the localised mixture deflagration overpressure (10) does not reduce to that for uniform mixture, i.e. $\Delta\pi = A\,Br_t^{-B}$ [4,17], due to peculiarities of derivation process and additional assumptions specific for localized mixture deflagrations.

For the analysis below the laminar burning velocity measurement [21] we accepted for hydrogen fractions above $\varphi_{H2} = 0.10$ and the measurements [22] below that value (value $S_{u0} = 0.11$ m/s was accepted at $\varphi_{H2} = 0.10$). Expansion ratio dependence on hydrogen concentration was calculated using thermodynamic equilibrium model.

3.2 Deflagration-outflow interaction number χ/μ

In this work calculation of deflagration-outflow interaction (DOI) number (i.e. overall flame wrinkling factor) is calculated similar to [17] as a product of individual flame wrinkling factors each describing its own phenomena contributing to flame acceleration: $\chi/\mu = \Xi_K\cdot\Xi_{LP}\cdot\Xi_{FR}\cdot\Xi_{u'}\cdot\Xi_{AR}\cdot\Xi_O$. Flame wrinkling factors $\Xi_K, \Xi_{LP}, \Xi_{FR}, \Xi_{u'}$ are a legacy of studies on CFD modelling and LES of hydrogen-air deflagrations conducted about last decade at Ulster, see e.g. [16, 24, 25].

The flame wrinkling due to turbulence generated by flame front itself, Ξ_K, is based on considerations developed by Karlovits et al. [26]. The upper value of the factor was shown to be equal to $\Xi_K^{\max} = (E_i - 1)/\sqrt{3}$ [27]. In the present lumped parameter model the wrinkling factor is equal to $\Xi_K = \psi\,\Xi_K^{\max}$, where ψ is the tuning coefficient reflecting Karlovitz' observation that the maximum value of the turbulence generated by the flame front itself was not realised all the time and adopted here as follows: $\psi = 1$ for $\varphi < 0.2, \psi = -5\varphi + 2$ for $0.2 \le \varphi \le 0.3$, and $\psi = 0.5$ for $\varphi > 0.3$.

The leading point wrinkling factor Ξ_{LP} describes flame acceleration due to the preferential diffusion effect in so called "leading points" of wrinkled flame, particularly pronounced in lean hydrogen-air mixtures. The wrinkling factor is calculated following Zimont and Lipatnikov [28], who found its value for different hydrogen concentrations. In the present study the factor is approximated as a function of hydrogen concentration, $\Xi_{LP}^{\max} = 6.3\varphi^2 - 7.5\varphi + 3.0$.

The wrinkling factor Ξ_{FR} accounts for combustion augmentation due to fractal nature of the flame front. Gostintsev et al. [29] suggested that transition from cellular to fully turbulent self-similar regime of flame propagation occurs after critical flame radius R_0. In the presented model the flame wrinkling factor is modelled as $\Xi_{FR} = 1.0$ for $R \le R_0$, and $\Xi_{FR} = \left(R / R_0\right)^{D-2}$ for $R > R_0$, where the critical radius is believed to be a function of hydrogen concentration in a flammable mixture: $R_0 = 4.3478\,\varphi - 0.2826$ for $\varphi \le 0.295$ and $R_0 = 1.0\,\text{m}$ for $\varphi > 0.295$. The dependence is fitted to provide critical radius value $R_0 = 1.0\,\text{m}$ in agreement with Gostintsev et al. [29], who reported the critical value $R_0 = 1.0 - 1.2\,\text{m}$ for near stoichiometric hydrogen-air mixtures, and to decrease in lean mixtures reflecting their higher susceptibility to thermodiffusive and hydrodynamic instabilities. Fractal dimension value was adopted as $D = 2.33$ [30]. Application of fractal wrinkling factor requires knowledge of maximum characteristic flame size, which was taken here as enclosure length – $R = 1.0$ m for KIT experiments and $R = 5.0\,\text{m}$ for the HSL experiment.

Wrinkling factor $\Xi_{u'}$ accounts for the effect of initial flow turbulence on flame propagation. In all considered experiments the mixture was initially quiescent and the factor was taken as $\Xi_{u'} = 1.0$.

Premixed flame propagating through an enclosure tends to elongate towards a vent and eventually takes the shape of enclosure. The aspect ratio flame wrinkling factor Ξ_{AR} accounts for the growth of flame front area due to its elongation in enclosures. In the present work the aspect ratio wrinkling factor was calculated as the ratio of area of total burnt mixture (occupying volume $\Phi E_i V$ under enclosure ceiling) to the area of sphere having the same volume as burnt mixture.

Flame wrinkling factor Ξ_O models flame acceleration due to wrinkling and turbulisation of flame by obstacles. No obstacles were employed in the considered experimental program, hence $\Xi_O = 1.0$.

3.3 Processing non-uniform localised mixture results

Application of correlation (9) for venting deflagrations of non-uniform layer requires criteria for specification of layer fraction Φ contributing to pressure build-up. In this work the volume fraction of hydrogen-air layer Φ is calculated as a ratio of the layer thickness, containing mixture with the burning velocity within a specified range of the maximum burning velocity $S_{u_{MAX}}$, to the whole vessel height. The ranges of maximum burning velocity $(0.8-1.0)S_{u_{MAX}}$, $(0.9-1.0)S_{u_{MAX}}$, $(0.95-1.0)S_{u_{MAX}}$, and $(0.98-1.0)S_{u_{MAX}}$ were tested. It was also assumed that flame does not propagate in downward direction when hydrogen fraction in the mixture is below $\varphi_{H2} = 0.095$, and combustible mixture fraction Φ was limited by this threshold value as well. Mixture properties were calculated as a function of average hydrogen concentration in the considered portion of the layer $\bar{\varphi} = (\varphi_{MAX} + \varphi_{MIN})/2$. The best agreement between uniform and non-uniform mixture deflagration overpressures was obtained for the burning velocity range $(0.95-1.0)S_{u_{MAX}}$. This result is in line with the analytical expression for overpressure (8), which may be used to show that maximum deflagration overpressure is dominated by fastest burning mixture with maximum expansion coefficient. Hydrogen distribution together with distribution of burning velocity in non-uniform mixtures and value of Φ corresponding to the range $(0.95-1.0)S_{u_{MAX}}$ is given in Table 1 for KIT experiments, and in Table 2 for the HSL experiment. The value of Φ for the most considered experiments is as low as 2.66% -3.71%, with the largest value in

experiments with Gradient 6 mixtures (HIWP3-032, HIWP3-045, see Table 1 below), where combustible fraction is just Φ=9%.

Table 1. Mixture properties in KIT experiments, burning velocity range $(0.95-1.0)S_{u_{MAX}}$.

	Gradient 1			**Gradient 2**			**Gradient 3**		
Height, m	H_2 fraction, % (vol.)	Burning velocity S_u, m/s	Φ	H_2 fraction, % (vol.)	Burning velocity S_u, m/s	Φ	H_2 fraction, % (vol.)	Burning velocity S_u, m/s	Φ
1.00	11.98	0.140	$3.71\cdot10^{-2}$	14.95	0.362	$2.71\cdot10^{-2}$	16.98	0.544	$2.71\cdot10^{-2}$
0.75	9.87	0.093		12.71	0.195		14.09	0.292	
0.50	6.23	0.051		8.60	0.130		9.31	0.100	
0.25	3.21	0.0		5.05	0.0		5.41	0.047	
0	2.11	0.0		3.55	0.0		3.77	0.0	
	Gradient 4			**Gradient 5**			**Gradient 6**		
Height, m	H_2 fraction, % (vol.)	Burning velocity S_u, m/s	Φ	H_2 fraction, % (vol.)	Burning velocity S_u, m/s	Φ	H_2 fraction, % (vol.)	Burning velocity S_u, m/s	Φ
1.00	16.94	0.540	$2.66\cdot10^{-2}$	20.00	0.857	$2.81\cdot10^{-2}$	10.00	0.100	$9.00\cdot10^{-2}$
0.75	14.01	0.286		16.25	0.475		9.13	0.090	
0.50	10.19	0.100		11.00	0.125		7.75	0.055	
0.25	6.69	0.053		6.38	0.052		6.44	0.052	
0	5.22	0.0		4.63	0.0		5.88	0.050	

Table 2. Mixture properties in HSL experiment, burning velocity range $(0.95-1.0)S_{u_{MAX}}$.

Height, m	H_2 fraction, % (vol.)	Burning velocity S_u, m/s	Φ
2.50	12.96	0.211	$3.48\cdot10^{-2}$
2.17	12.32	0.172	
1.86	12.01	0.154	
1.55	11.22	0.119	
1.24	10.17	0.105	
0.93	7.91	0.058	
0.62	2.57	0.0	
0.31	0.13	0.0	

4.0 RESULTS AND ANALYSIS FOR LOCALISED MIXTURE DEFLAGRATION VENTING

Experimental data from KIT and HSL deflagrations were processed as described above. Figure 1 gives comparison between experimental results and overpressure predictions (10) with the best fit coefficients A=0.018 and B=0.94 obtained for the range $(0.95-1.0)S_{u_{MAX}}$. The same results are given in **Error! Reference source not found.** with major mixture properties and calculation parameters. Experiments with non-uniform layered mixtures (**Error! Reference source not found.** entries 1-14 and 25) are shaded by grey colour for easier identification. The conservative fit (to compensate for underprediction in HSL WP3/Test22 test) is achieved with coefficients A=0.089 and B=0.94.

In uniform layers the largest experimental overpressures was obtained for deflagrations with largest hydrogen fractions - 25% (HIWP3-079 and -082) and 20% (HIWP3-076, -077, -078, -081) in spite of relatively large vent area 0.25 m^2. For the considered deflagrations in non-uniform mixtures the largest overpressures were also achieved where hydrogen fractions are the largest - 20% (HIWP3-038), 17% (HIWP3-035, -036, -037, -041, -0.42, -0.43), and 15% (HIWP3-034, -044).

In Figure 1 the non-uniform layer results have larger scatter between predicted and experimental data. The largest error here is 189% (overprediction) for the test HIWP3-032 (Φ=0.09, φ=0.10), and the largest scatter between maximum and minimum error is 225%. For uniform layers the largest error is 146% (overprediction) for the test HIWP3-074 (Φ=0.25, φ=0.15), and the largest scatter is 223%.

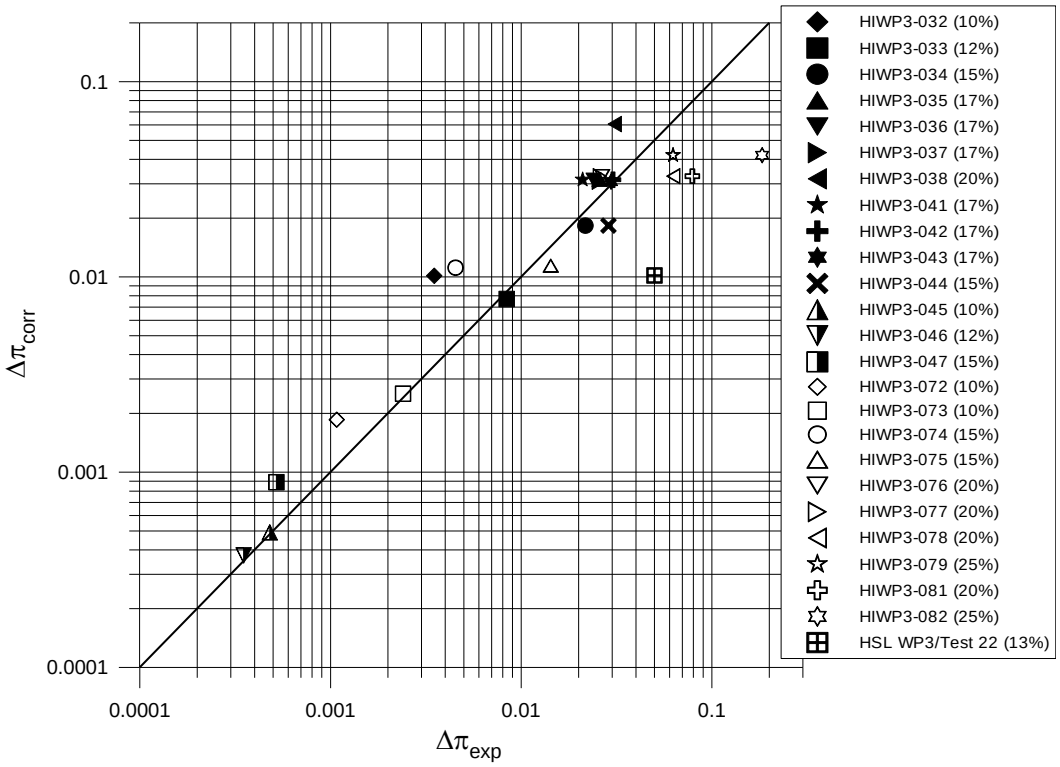

Figure 1. Comparison between experimental and correlated overpressures.

Correlation overpressure for the test WP3/Test22 by HSL with non-uniform layer is lower than the rest of the non-uniform layer data. The experimental overpressure $5.0\cdot10^{-2}$ bar is a filtered value here (non-filtered value is $6.0\cdot10^{-2}$ bar). Calculated overpressure is $1.02\cdot10^{-2}$ bar, which is underprediction by -80%. Having data just for one test in HSL facility it is difficult to speculate about the nature of such a discrepancy - whether it is a general data scatter, effect of scale, or peculiarity of the experiment. Reviewing WP3/Test22 data and model parameters does not reveal areas having potential to significantly increase this value.

Generally the proposed correlation performed reasonably well on the available for comparison set of experimental data. Wider range of experimental conditions in terms of vessel size, vent area, mixture fraction Φ and hydrogen fraction φ is required to test the proposed theoretically based correlation and the technique to treat non-uniform mixture layers.

5.0 CONCLUSIONS

A series of experiments on vented layered deflagration of uniform and stratified hydrogen-air mixtures was performed at KIT (Germany) and HSL (UK). Maximum combustion pressure in an enclosure was measured as integral characteristic of combustion process as function of hydrogen concentration gradient and vent area for two different scales 1 and 31 m^3.

The analytical model for vented deflagration of localised mixtures and its major assumptions and simplifications were demonstrated. The model is applicable for protection of low strength structures and buildings, where level of overpressures is below 1 bar.

Table 3. Model parameters and results of overpressure correlation (10) with the best fit coefficients A=0.018 and B=0.94

	Experiment	Layer	Vent area, m^2	Φ, % (vol.)	$\overline{\varphi}$, % (vol.)	R_0, m	E_i	M_u, kg/kmol	S_{ui}, m/s	c_{ui}, m/s	Ξ_K	Ξ_{LP}	Ξ_{FR}	Ξ_{AR}	χ/μ	Br_t^{-1}	$\left(\frac{E_i}{\sqrt{2}}\right)^{1/2} MIN\{1.0; E_i^{2/3} n^{2/3}\}$	$\Delta\pi_{exp}$	$\Delta\pi_{corr}$
1	HIWP3-032	Gradient 6	0.01	9.00	9.8	0.15	3.47	26.20	0.095	361	1.42	2.32	1.89	1.46	9.1	1.81	0.568	$3.50\cdot10^{-3}$	$1.01\cdot10^{-2}$
2	HIWP3-033	Gradient 1	0.01	3.71	11.8	0.23	3.90	25.67	0.138	365	1.67	2.20	1.62	1.93	11.5	3.66	0.356	$8.40\cdot10^{-3}$	$7.71\cdot10^{-3}$
3	HIWP3-034	Gradient 2	0.01	2.71	14.8	0.36	4.53	24.86	0.336	370	2.04	2.03	1.40	2.08	12.1	10.32	0.337	$2.17\cdot10^{-2}$	$1.83\cdot10^{-2}$
4	HIWP3-035	Gradient 3	0.01	2.71	16.8	0.45	4.92	24.32	0.508	374	2.26	1.92	1.30	2.00	11.3	15.51	0.365	$2.58\cdot10^{-2}$	$3.15\cdot10^{-2}$
5	HIWP3-036	Gradient 3	0.01	2.71	16.8	0.45	4.92	24.32	0.508	374	2.26	1.92	1.30	2.00	11.3	15.51	0.365	$2.40\cdot10^{-2}$	$3.15\cdot10^{-2}$
6	HIWP3-037	Gradient 4	0.01	2.66	16.8	0.45	4.91	24.33	0.504	374	2.26	1.92	1.30	2.02	11.4	15.51	0.360	$2.55\cdot10^{-2}$	$3.08\cdot10^{-2}$
7	HIWP3-038	Gradient 5	0.01	2.81	19.8	0.58	5.48	23.53	0.804	381	2.59	1.76	1.20	1.88	10.3	23.69	0.415	$3.09\cdot10^{-2}$	$6.06\cdot10^{-2}$
8	HIWP3-041	Gradient 3	0.01	2.71	16.8	0.45	4.92	24.32	0.508	374	2.26	1.92	1.30	2.00	11.3	15.51	0.365	$2.10\cdot10^{-2}$	$3.15\cdot10^{-2}$
9	HIWP3-042	Gradient 3	0.01	2.71	16.8	0.45	4.92	24.32	0.508	374	2.26	1.92	1.30	2.00	11.3	15.51	0.365	$3.03\cdot10^{-2}$	$3.15\cdot10^{-2}$
10	HIWP3-043	Gradient 4	0.01	2.66	16.8	0.45	4.91	24.33	0.504	374	2.26	1.92	1.30	2.02	11.4	15.51	0.360	$2.96\cdot10^{-2}$	$3.08\cdot10^{-2}$
11	HIWP3-044	Gradient 2	0.01	2.71	14.8	0.36	4.53	24.86	0.336	370	2.04	2.03	1.40	2.08	12.1	10.32	0.337	$2.87\cdot10^{-2}$	$1.83\cdot10^{-2}$
12	HIWP3-045	Gradient 6	0.25	9.00	9.8	0.15	3.47	26.20	0.095	361	1.42	2.32	1.89	1.46	9.1	0.07	0.568	$4.80\cdot10^{-4}$	$4.92\cdot10^{-4}$
13	HIWP3-046	Gradient 1	0.25	3.71	11.8	0.23	3.90	25.67	0.138	365	1.67	2.20	1.62	1.93	11.5	0.15	0.356	$3.50\cdot10^{-4}$	$3.74\cdot10^{-4}$
14	HIWP3-047	Gradient 2	0.25	2.71	14.8	0.36	4.53	24.86	0.336	370	2.04	2.03	1.40	2.08	12.1	0.41	0.337	$5.20\cdot10^{-4}$	$8.89\cdot10^{-4}$
15	HIWP3-072	Uniform	0.25	25.0	10.0	0.15	3.50	26.16	0.104	361	1.44	2.31	1.86	1.24	7.7	0.07	1.134	$1.07\cdot10^{-3}$	$1.86\cdot10^{-3}$
16	HIWP3-073	Uniform	0.25	50.0	10.0	0.15	3.50	26.16	0.104	361	1.44	2.31	1.86	1.24	7.7	0.07	1.323	$2.40\cdot10^{-3}$	$2.52\cdot10^{-3}$
17	HIWP3-074	Uniform	0.25	25.0	15.0	0.37	4.56	24.81	0.350	371	2.06	2.02	1.39	1.24	7.1	0.26	1.491	$4.52\cdot10^{-3}$	$1.12\cdot10^{-2}$
18	HIWP3-075	Uniform	0.25	50.0	15.0	0.37	4.56	24.81	0.350	371	2.06	2.02	1.39	1.24	7.1	0.26	1.510	$1.43\cdot10^{-2}$	$1.14\cdot10^{-2}$
19	HIWP3-076	Uniform	0.25	25.0	20.0	0.59	5.52	23.47	0.826	381	2.61	1.75	1.19	1.24	6.8	0.64	1.661	$2.66\cdot10^{-2}$	$3.28\cdot10^{-2}$
20	HIWP3-077	Uniform	0.25	25.0	20.0	0.59	5.52	23.47	0.826	381	2.61	1.75	1.19	1.24	6.8	0.64	1.661	$2.58\cdot10^{-2}$	$3.28\cdot10^{-2}$
21	HIWP3-078	Uniform	0.25	50.0	20.0	0.59	5.52	23.47	0.826	381	2.61	1.75	1.19	1.24	6.8	0.64	1.661	$6.27\cdot10^{-2}$	$3.28\cdot10^{-2}$
22	HIWP3-079	Uniform	0.25	25.0	25.0	0.80	6.36	22.13	1.24	393	2.32	1.52	1.07	1.24	4.70	0.72	1.783	$6.26\cdot10^{-2}$	$4.20\cdot10^{-2}$
23	HIWP3-081	Uniform	0.25	50.0	20.0	0.59	5.52	23.47	0.826	381	2.61	1.75	1.19	1.24	6.76	0.64	1.661	$7.90\cdot10^{-2}$	$3.28\cdot10^{-2}$
24	HIWP3-082	Uniform	0.25	50.0	25.0	0.80	6.36	22.13	1.24	393	2.32	1.52	1.07	1.24	4.70	0.72	1.783	$1.83\cdot10^{-1}$	$4.20\cdot10^{-2}$
25	WP3/Test22	Non-uniform	0.448	3.48	12.9	0.28	4.13	25.38	0.197	367	1.81	2.14	2.59	4.50	45.1	4.73	0.362	$5.00\cdot10^{-2}$	$1.02\cdot10^{-2}$

The model analysis suggests that only a small fraction of the mixture with closest to the stoichiometry composition will have decisive effect on the final overpressure of non-uniform mixture deflagrations. A technique to calculate this fraction of unburnt mixture in non-uniform layers was developed. The technique accounts a portion of the mixture having burning velocity within a specified range of the maximum burning velocity considered in deflagration scenario. For the tested range of hydrogen-air mixtures the best agreement with the experimental data and between uniform and non-uniform mixtures is achieved for the burning velocity range between 95% and 100% of the maximum burning velocity.

The model was successfully validated against KIT and HSL experiments. Coefficients for the vented deflagration correlation were fitted against 25 uniform and non-uniform mixture experiments performed at KIT (Germany) and at HSL (UK) facilities. Coefficients were obtained for the best fit, and conservative correlations. The obtained results are generally plausible and in a good agreement with the experimental data.

The developed model has a potential to be used for hazards analysis and design of mitigation measures against deflagrations of realistic non-uniform mixtures in context of safe indoor use of hydrogen installations.

ACKNOWLEDGEMENT

The authors are grateful to European Commission for supporting this research through FP7 FCH-JU project “Hyindoor” (“Pre-normative research on safe indoor use of fuel cells and hydrogen systems”), grant agreement No. 278534.

REFERENCES

1. Tamanini, F., “Partial-volume deflagrations – characteristics of explosions in layered fuel/air mixtures”, *Proc. 3rd Int. Seminar on Fire and Explosion Hazards (ISFEH3)*, Lake Windermere, England, pp.103-117 (2000).
2. Whitehouse, D.R., Greig, D.R., Koroll, G.W., “Combustion of stratified hydrogen-air mixtures in the 10.7 m3 combustion test facility cylinder”, Nuclear Engineering and Design 166:453-462 (1996).
3. Kuznetsov, M., Yanez, J., Grune, J., Friedrich, A., and Jordan, T., “Hydrogen Combustion in a Flat Semi-Confined Layer with Respect to the Fukushima Daiichi Accident”, Nuclear Engineering and Design, 286:36-48 (2015)
4. Molkov, V.V., “Unified correlations for vent sizing of enclosures at atmospheric and elevated pressures”, J. Loss Prev. Process, 14:567-574 (2001).
5. Kuznetsov, M., Grune, J., Friedrich, A., Sempert, K., Breitung, W., and Jordan, T., “Hydrogen-Air Deflagrations and Detonations in a Semi-Confined Flat Layer”, In: Fire and Explosion Hazards, Proceedings of the Sixth International Seminar (Edited by D. Bradley, G. Makhviladze and V. Molkov), pp.125-136 (2011).
6. Grune, J., Sempert, K., Haberstroh, H., Kuznetsov, M., and Jordan, T., “Experimental Investigation of Hydrogen-Air Deflagrations and Detonations in Semi-Confined Flat Layers”, Journal of Loss Prevention in the Process Industries, 26(2):317-323 (2013).
7. Grune, J., Sempert, K., Kuznetsov, M., Jordan, T., “Experimental investigation of fast flame propagation in stratified hydrogen–air mixtures in semi-confined flat layers”, Journal of Loss Prevention in the Process Industries, 26(6):1442-1451 (2013).
8. Rudy, W., Kuznetsov, M., Porowski, R., Teodorczyk, A., Grune, J., Sempert, K., “Critical conditions of hydrogen–air detonation in partially confined geometry”, Proceedings of the Combustion Institute, 34(2):1965-1972 (2013).

9. Yao C., “Explosion-venting of low-strength equipment and structures”, Int. J. Loss Prevention, 8:1-9 (1974).
10. Pasman, H.L., Groothuizen, Th.M., de Gooijer, H., “Design of pressure relief vents”. In: Loss Prevention and Safety Promotion in the Process Industries, Ed. by C.H. Bushman, pp.185-189 (1974).
11. Bradley, D., Mitcheson, A., “The venting of gaseous explosions in spherical vessels”, Combustion and Flame, 32:221-236 and 237-255 (1978).
12. Molkov, V.V., Nekrasov, V.P., “Dynamics of gaseous combustion in a vented constant volume vessel”. Combustion, Explosion and Shock Waves, 17(4):363-370 (1984).
13. Razus, D.M., Krause, U., “Comparison of empirical and semi-empirical calculation methods for venting of gas explosions”. Fire Safety Journal, 36:1-23 (2001).
14. Bauwens, C.R., Chaffee, J., Dorofeev, S.B., “Effect of ignition location, vent size and obstacles on vented explosion overpressure in propane-air mixtures”, Combust. Sci. Tech. 182 (11):1915-1932 (2010).
15. Bauwens, C.R., Chao, J., Dorofeev, S.B. , “Evaluation of a multi peak explosion vent sizing methodology”, *Proc. 9th Int. Symposium on Hazards, Prevention and Mitigation of Industrial Explosions, Krakow, Poland, 22-27 July 2012* (2012).
16. Molkov, V., *Fundamentals of hydrogen safety engineering*, Vol.II, Bookboon.com, 2012, ISBN 978-87-403-0226-4.
17. Molkov, V., Bragin, M., “Hydrogen-air deflagrations: vent sizing correlation for low-strength equipment and buildings”, *Proc. 7th Int. Seminar on Fire and Explosion Hazards (ISFEH7), Providence, RI, USA, 5-10 May 2013* (2013).
18. Jallais S., Kudriakov S., “An inter-comparison exercise on engineering models capabilities to simulate hydrogen vented explosions”, *Int. Conf. Hydrogen Safety, Brussels, Belgium, 9-11 September 2013* (2013).
19. NFPA 68 “*Guide for Venting of Deflagrations. National Fire Protection Association”*, Quincy, MA, USA (1998).
20. Molkov V., *Venting gaseous deflagrations*, DSc Thesis, VNIIPO, Moscow, 1996 (in Russian).
21. Lamoureux, N, Djebaili-Chaumeix, N, Paillard, C.-E., “Flame velocity determination for H2-air-He- CO2 mixtures using the spherical bomb”, Experimental Thermal and Fluid Science 27:385-393 (2003).
22. Ross, M.C., *Lean Combustion Characteristics of Hydrogen-Nitrous Oxide-Ammonia Mixtures in Air*, Engineer’s thesis, California Institute of Technology (1997) (http://resolver.caltech.edu/CaltechETD:etd-01182008-143226)
23. Babkin, V.S., Private communication. Institute of Chemical Kinetics and Combustion, Siberian Branch, Russian Academy of Science, Novosibirsk, Russia (2003).
24. Verbecke, F., *Formation and combustion of non-uniform hydrogen-air mixtures*. PhD Thesis,University of Ulster, Belfast, UK (2009).
25. Xiao, H., Makarov, D., Sun, J. and Molkov, V., “Experimental and numerical investigation of premixed flame propagation with distorted tulip shape in a closed duct”. Combustion and Flame, 159:1523-1538 (2012).
26. Karlovitz, B., Denniston, D.W.Jr., Wells, F.E., “Investigation of turbulent flames”, The Journal of Chemical Physics 19(5):541-547 (1951).
27. Molkov, V.V., Nekrasov, V.P., Baratov, A.N., Lesnyak, S.A., “Turbulent gas combustion in a vented vessel”, Combustion, Explosions and Shock Waves, 20:149-153 (1984).
28. Zimont, V.L., Lipatnikov, A.N., “A numerical model of premixed turbulent combustion of gases”, Chem. Phys. Reports 14(7): 993-1025 (1995).
29. Gostintsev, Yu.A., Istratov, A.G., Shulenin, Yu.V., “Self-similar propagation of a free turbulent flame in mixed gas mixtures. Combustion”, Explosion and Shock Waves 24(5):63-70 (1988).
30. Bradley, D., “Instabilities and flame speeds in large scale premixed gaseous explosions”, Phil.Trans. R.Soc. London A., 357:3567-3581 (1999).